THE EFFECT OF CREEP STRAIN RATE ON DAMAGE ACCUMULATION IN TYPE 316H AUSTENITIC STAINLESS STEEL

E.A. Hares, M. Mostafavi, R. Bradford and C.E. Truman
Department of Mechanical Engineering, University of Bristol, UK

Abstract: Many service components in power generation and aerospace industries operate at high temperatures and stresses that make them susceptible to creep deformation and damage. Their complex geometries and load multi-axiality are often treated only approximately in assessing their structural integrity via assessment codes that are based on standard creep tests. For example, the forward creep (defined here as constant load creep) test of round bars is not a true representation of the stress state that service components generally experience. The experiments conducted in this work used notched bar specimens to simulate the effect of stress triaxiality. The results from these experiments were then used to validate a well-established creep ductility exhaustion damage model. Although the damage model is largely based on uniaxial creep rupture tests, it has been previously adapted so that it can be applied to more complex states of stress. Rupture calculations were conducted prior to experimental testing to obtain an estimation of the duration of the experiments. The finite element simulation results, which utilised previously developed creep deformation and damage models, were then compared to the experimental data. It was shown that the model predicted the correct trend for the creep deformation and failure of the specimens and primary, secondary and tertiary creep behaviour of notched bars could be captured. The tests imply that the effective creep ductility was smaller at lower stresses, i.e., at slower strain rates creep strain was more damaging.

1. Introduction

Stainless steel is commonly used in the fabrication of components in the power generation industry. These components are subjected to high temperature creep during plant operation, typically at 550˚C, and therefore it was important to evaluate their behaviour in the creep regime. Both creep deformation and creep damage play a significant role in the fitness for service of such components. Creep damage is a phenomenon that occurs in metals after prolonged exposure to high stress and high temperature and it can lead to catastrophic failure. It can initiate early in operation and develop gradually throughout the life of a component [1, 2]. The main aim of this research was to determine whether creep strain is more damaging to a specimen if accumulated more slowly. A model capable of forecasting creep damage correctly within a material/component can be used to estimate its creep life. With an increasing need to extend the lives of UK nuclear power plants, it is important to be able to accurately predict when failures are likely to occur so that safe operation can be achieved. It has been observed that the current methods for forecasting the accumulation of creep damage tend to be very conservative [3, 4], whereas the more modern technique reported in this work is thought to be more accurate, but has not been implemented extensively.

Uniaxial stress relaxation behaviour has been investigated in previous research by Spindler [5]. Uniaxial loading conditions are not truly representative of plant operating conditions because complex geometries and loading conditions are often present. Notched bar tests have been conducted by previous researchers to determine the multiaxial effect on creep ductility [6-8], defining creep ductility as the creep strain on failure. In this research notched bar specimens have been used to introduce a stress triaxiality [4, 9-11]. The degree of triaxiality of the stress state is defined through a stress triaxiality factor, η, defined as:

Equation 1

$$\eta = \frac{\sigma_p}{\bar{\sigma}}$$

where σ_p is the hydrostatic stress and $\overline{\sigma}$ is the von Mises equivalent stress. A high stress triaxiality factor accelerates structural degradation of components [11]. Ductility exhaustion, which is affected by the stress triaxiality factor, is postulated to be a governing factor in creep failure [12]. Consequently, it is important to evaluate the effects of notches on the creep deformation and damage for more realistic prediction of service components life.

Takahashi et al [13] conducted tests at 550˚C on notched bar specimens fabricated from Type 316FR stainless steel, a similar material to the one used in this study. They found that with an increase in net section stress the time to rupture was exponentially reduced. With a notch acuity of 2 (notch acuity is defined as a/R where a is the radius of specimen at the notched section and R is the radius of the notch) and a net section stress of 353MPa the time to rupture was 218 hours. Using an identical specimen with a net section stress of 245MPa the time to rupture was 94,177 hours. They found that extension of the specimens on failure increased with an increase in net section stress. With a net section stress of 353MPa the extension on failure was 39% and with a net section stress of 245MPa the extension on failure was 28%, these extension values did not include the loading phase (plastic strain). These results also showed a greater reduction in cross sectional area of the specimens at the notch with increased net section stress. The reduction of area at the notch on failure for the test with a net section stress of 353MPa was 52% and 45% with a net section stress of 245MPa. These values for reduction in area did not include plastic loading strain.

Spindler derived an empirical equation from multi-axial creep data of Type 316 stainless steel that incorporates cavity nucleation within creep behaviour[14]. The damage model presented is:

Equation 2:

$$\frac{\bar{\varepsilon}_f}{\varepsilon_{fu}} = \exp\left[p\left(1-\frac{\sigma_1}{\overline{\sigma}}\right)\right]\exp\left[q\left(\frac{1}{2}-\frac{3\sigma_p}{2\overline{\sigma}}\right)\right]$$

Where $\bar{\varepsilon}_f$ and ε_{fu} are the von Mises equivalent and uniaxial strains to failure, respectively. σ_1, $\overline{\sigma}$ and σ_p are the maximum principal, von Mises equivalent and hydrostatic stresses, respectively. p and q are constants based on the material and test temperature. They were calibrated to give the best fit for Type 316 stainless steel at 550˚C using notched bars with a notch acuity 5 in previous research conducted by Spindler[15]. The values of p and q established by Spindler were 1.2 and 1.0 respectively for the material used in this study.

Similar methods for assessing creep rupture of notched bars fabricated from Type 316H stainless steel at 550˚C have been conducted by previous researchers [2, 15]. Chang-Sik Oh et al achieved this by implementing a model incorporating ductility exhaustion [16, 17]. In this model when damage becomes unity at a gauss point all the stress components are reduced to a small value to simulate progressive failure. This model was found to have good agreement with experimental data.

The main aim of these experiments was to determine whether creep strain accumulated at different rates was equally damaging to the specimens. Another aim was to investigate how introducing a stress triaxiality affects the level of damage accumulation. These experiments were also conducted to investigate whether the deformation and onset of damage could be predicted in notched bar rupture tests. The deformation and damage were simulated using the Spindler damage function and the uniaxial creep constants for this material cast. Previous research found that failure strain depends on the stress state [18].

2. Methodology

2.1. Experimental

Existing data for forward creep tests (constant load creep tests) with un-notched specimens was used to obtain the primary and secondary creep constants for the specific cast [4, 14, 19, 20]. Primary creep was of the form [21]:

Equation 3

$$\varepsilon_p = A\sigma^n t^m$$

And secondary creep rate of the form:

Equation 4

$$\dot{\varepsilon}_S = C\sigma^{n_1}$$

Forward creep tests were then conducted on notched bar specimens to investigate how introducing a stress triaxiality affects the level of damage accumulated. It was ensured that the plain bar specimens endure the same level of stress that the notched specimens experience on average across the ligament. It can therefore be expected that any change in the creep behaviour of notched specimens is attributed to the notch, including the increased stress triaxiality factor.

Standard dead weight creep machines were used to conduct tests at 550°C. Two different types of creep rig were used; one design was automatically levelled and the other manually levelled. The automatically controlled test rigs were connected to capstans that kept the lever arms horizontal during a creep test. The manually levelling rigs were adjusted in accordance to the spirit levels attached to them. On both rig designs the specimens were connected at the middle of the rig and attached to the lever arm at the top of the specimen, and a 25kN load cell at the bottom. On the manually controlled rigs the load cell was attached to the manual levelling device and on the automatic rigs it was connected to the capstan. The load cell, which was at the base of the rigs, and connected to the data logger, measured the applied load. Thermocouples measured the temperature at the top, middle and bottom of the sample together with the room temperature.

The extension of the gauge length of the specimens (28.25mm) was measured using an extensometer and linear variable differential transformer (LVDTs). On two tests the specimen diameter was also measured. A diametric extensometer provided a measurement at the notch. A data logger captured temperature, load and extension data throughout the test together with diameter when available. As an alternative to the diametric extensometer a camera system allowed measurement of the complete notch profile. A USB camera (Logitech C270, 1280 X720 pixels) was adapted to take a zoom lens (Tokina TV lens 7900754, 1:2.5/22-88mm) and imaged the specimen though a 14mm diameter hole in the furnace. The sample was illuminated with a ring of light emitting diodes positioned around the optical axis. The camera was read out into a laptop and images were captured every 5 minutes. Analysis of these images provided the diameter of the specimen and the notch together with the notch profile throughout the test. The camera set up is shown in Figure 1. A focusing lens was attached to a simple webcam. This method was chosen because the images from the camera allowed the reduction in notch diameter, the notch opening and deformation of the specimen to be measured.

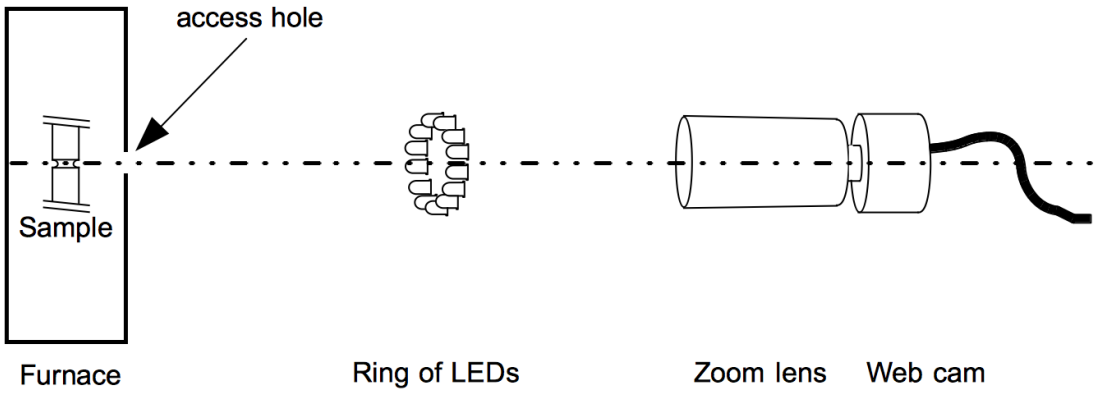

Figure 1 - Camera set up for notch imaging

The material, from which the specimens were fabricated, was a single cast of Type 316H austenitic stainless steel (internally referred to as cast 69431). The plant item from which the material was extracted has previous service history during which it was subject to temperatures between 480˚C and 510˚C for 50,000 hours. This caused thermal aging which altered its creep characteristics, details of which are described elsewhere [22, 23]. The material was chosen because there was existing uniaxial creep data for this material [5, 24]. The chemical composition of the material is shown in Table 1.

Table 1 - Chemical Composition of the Type 316H in Weight Percentage [15]

Element	C	Si	Mn	S	P	Ni	Cr	Mo	Co	B
wt%	0.06	0.4	0.98	0.014	0.021	11.83	17.17	2.19	0.1	0.05

Creep tests of circumferentially notched bar specimens were performed and compared with existing data for plain bar specimens to obtain strain time data with stress triaxiality for a single cast of Type 316H austenitic stainless steel. It is important to note that the variation of creep behaviour between different casts can be significant and the use of a single cast was deliberate to remove this source of scatter. All cylindrical specimens were machined to meet codes of practice for conducting experiments with notched bars [25]. Dimensions are shown graphically in Figure 2 and stated in Table 2. All specimens had a notch acuity of 5 [18, 24, 26] This was to ensure that the notch was sharp enough to create an increased stress triaxiality and still within machining limits.

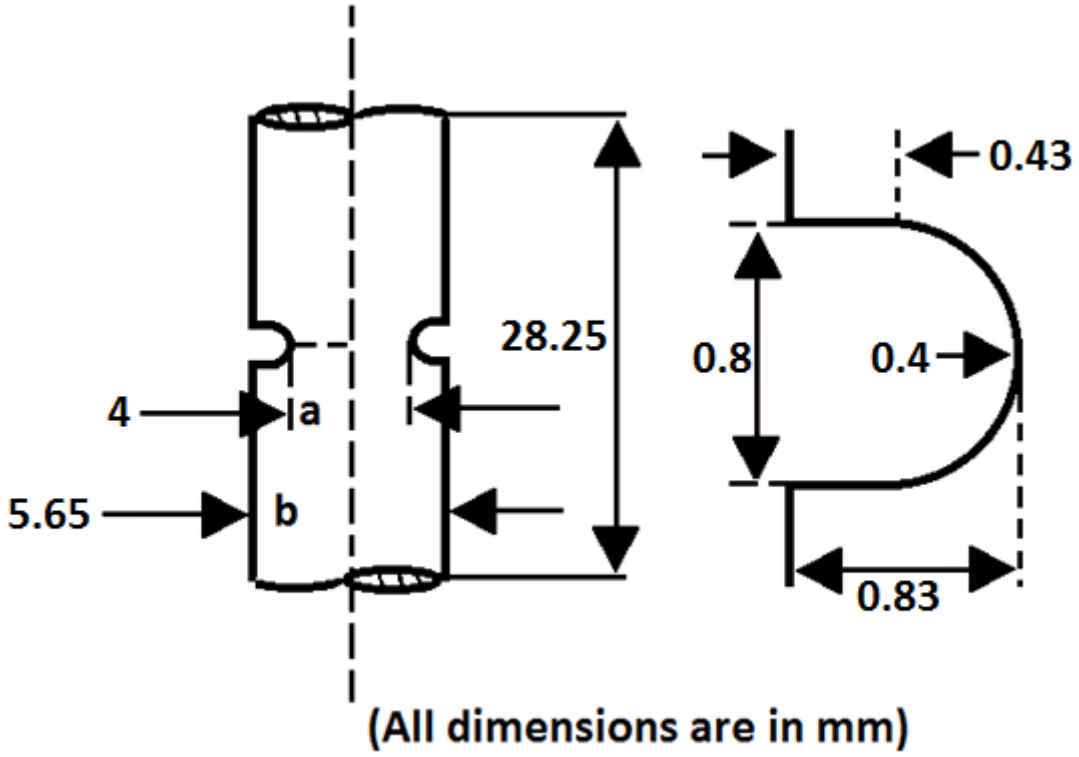

Figure 2- Specimen Dimensions (tolerances of 0.01mm for machining)

Table 2 - Specimen Dimensions

Notch Acuity (a/R)	R (mm)	a (mm)	b (mm)	L (mm)
5	0.4	2	2.83	28.25

Where R was the radius of the notch, a was the radius of the specimen at the notch, b was the radius of the specimen away from the notch and L was the gauge length of the specimen.

2.2. Numerical analysis

Finite element simulations were conducted using Abaqus version 6.14 [27]. Initial simulations were conducted on a round bar specimen to ensure that elastic and plastic loading conditions could be accurately captured in the model. These simulations were compared with experimental data for the load up of uniaxial creep tests at varying stresses. Then primary and secondary creep were added to the model and again validated against experimental data.

The next step of the simulation was introducing the notched specimen used in the tests conducted for this research. A mesh sensitivity study found that the elements at the notch tip needed to be 0.01mm or smaller for the result to be mesh independent. Approximately 1000 structured quadratic elements were used. The part was axisymmetric, a further plane of symmetry was added along the centre line of the notch. The load was applied as a constant pressure on the top edge of the specimen. The analysis was conducted assuming ‘large displacements’ (NLGEOM ON) since the notch geometry changes substantially under load.

Modelling creep of notched bars was done via employing a user subroutine to incorporate the empirical constants for primary and secondary creep. Tertiary creep was simulated by factoring the nominal strain rate by $1/(1-D_C^3)$ using the Spindler damage model, where D_C is the damage defined by equation 5, below. This factor has been implemented successfully in previous research by Spindler on this material [28]. The Spindler damage model was based on ductility exhaustion and the triaxiality factor given by equation 2. These simulations were used to determine the stress, strain and damage across the notched section.

The following constants were used:

Table 3 - Constants used in finite element simulations

E (MPa)	ν	A	n	m	C	n_1	Uniaxial Ductility, ε_{fu}
165,000	0.3	1.84E-12	4.5	0.421	2.49E-27	9.17	10.7%

(Units of A and C are such that strain rates result in absolute per hour for stress in MPa and time in hours).

where E and ν were the Young's modulus and Poisson's ratio for material at 550˚C respectively, (obtained from a tensile test on this material at 550˚C). A, n and m were the primary creep constants, and C and n_1 were the secondary creep constants. These were calculated from experimental data on round bars fabricated from the same component and cast of 316H [24]. The elastic-plastic stress-strain response values were taken from a tensile test for this material at 550˚C conducted within this work according to ASTM [29]. A creep damage function was added to the user subroutine so that tertiary creep and damage could be accounted for in the model. This was calculated using ductility exhaustion, as shown in equation 5.

Equation 5

$$D_C = \frac{\bar{\varepsilon}_c}{\bar{\varepsilon}_f}$$

where $\bar{\varepsilon}_c$ was the accumulated von Mises creep strain and $\bar{\varepsilon}_f$ was given by equation 2.

Two different failure cases were modelled. In the first case failure was deemed to have occurred when the node of maximum damage reached a D_C value of 1. In this work these failures were referred to as the Type 1 failure criterion. In the second case failure was deemed to have occurred when all nodes along the line of symmetry going through centre line of the notch reached a D_C value of 1. These were referred to as the Type 2 failure criterion. When elements reach a damage value of 1 (unity) the damage level does not increase any more, but the creep strain continues to increase towards infinity and so the load held by these elements falls and the stress is concentrated elsewhere, similar to methods used by previous researchers to simulate progressive failure [16, 17] (in these similar methods the material modulus and yield stress also reduce as damage occurs, though this does not apply here). This causes an effect similar to that of the elements losing stiffness. This is an approximate allowance for the initiation and propagation of a crack, although the crack tip field is not modelled.

3. Results

3.1. Experimental

The results of the tests are reported in Table 4 and shown graphically in Figures 4 to 7. Nine creep rupture tests were conducted on notched bar specimens with various stresses and a notch acuity of 5. The test with a net section stress of 260MPa was interrupted by a power cut which resulted in the structural integrity of the specimen being lost.

Table 4 - Experimental results (test at 260MPa was interrupted by a power cut which led to damage of specimen)

Net Section Stress (MPa)	Rupture Time	E_0 (mm)	E_f (mm)	d_0 (mm)	d_f (mm)	ε_h (abs)	$\bar{\varepsilon}_{skf}$ (abs.)
260	>4320	0.055	-	3.95	-	-	-
342	11097	0.11	0.43	3.91	3.79	-0.0312	0.0391
390	480	0.29	0.60	3.80	3.70	-0.0267	0.0334
432	175	0.58	1.00	3.80	3.68	-0.0321	0.0402
436	307	0.70	1.19	3.63	3.54	-0.0251	0.0315
469	231	0.41	0.84	3.60	3.46	-0.0397	0.0497
500	16	1.18	1.73	3.65	3.51	-0.0391	0.0490
500	23	-	-	3.82	3.61	-0.0565	0.0708
515	35	0.56	1.13	3.49	3.32	-0.0499	0.0625

E_0 and E_f were the extension after initial loading and on failure respectively. d_0 and d_f were the diameter after initial loading and on failure respectively (the diameter and extension after load-up were measured so that contraction/extension due to plasticity and creep could be separated). ε_h was the surface hoop creep strain. For a notched bar this was calculated using the following expression (noting that it is the hoop strain which is related to the measured diameter of the specimens. The diameter after initial load-up, d_0, was used so that the creep strain could be isolated):

Equation 6

$$\varepsilon_h = \ln\left(\frac{d_f}{d_0}\right)$$

$\bar{\varepsilon}_{skf}$ was the skeletal Mises strain on failure. It has been determined in previous work that for a notched bar with notch acuity 5 that $\bar{\varepsilon}_{skf}/\ \varepsilon_h$=-1.253 [24]. This value was validated within the finite element analysis conducted within this work. It was found that after 300 hours of creep with a net section stress of 350MPa $\bar{\varepsilon}_{skf}$ was 3.9E-3 and ε_h was -3.1E-3, these values agreed with the conversion factor calculated previously by Spindler. The skeletal point is the point where the stress state is insensitive to the power law stress dependence of creep. It is often used as the point of analysis in notched bar testing [30].

The rupture time reduced with an increase in net section stress as shown in Figure 3a, the maximum time to rupture was 11097 hours with a net section stress of 342MPa, the minimum time to rupture was 23 hours with a net section stress of 500MPa. The diameter on failure reduced with an increase in net section stress, this can be seen graphically in Figure 3b. The maximum diameter on failure was on the lowest stress completed test, the diameter was 3.79mm on failure with a net section stress of 342MPa and the smallest diameter on failure was from the highest stress test, 3.32mm on failure at a net section stress of 515MPa. The relation between diameter on failure and net section stress was a linear relationship with every 1MPa

of stress added the diameter on failure was reduced by 0.0026mm. Extension during creep was increased with an increased net section stress as highlighted in Figure 3c. The maximum extension during creep was 0.57mm and the minimum was 0.31mm. The relationship between overall specimen extension during creep and net section stress was linear, with every 1MPa of stress added the increase in length of specimen during creep was 0.0016mm. Figure 4 shows the time to rupture for various net section stresses. Figure 5 shows the creep ductility on failure for the notched specimens (with a/R=5), defined as the skeletal point Mises creep strain, as well as the creep ductility on failure for uniaxial specimens with the same cast, conducted in previous research [24]. The uniaxial specimens had a significantly larger creep ductility on failure.

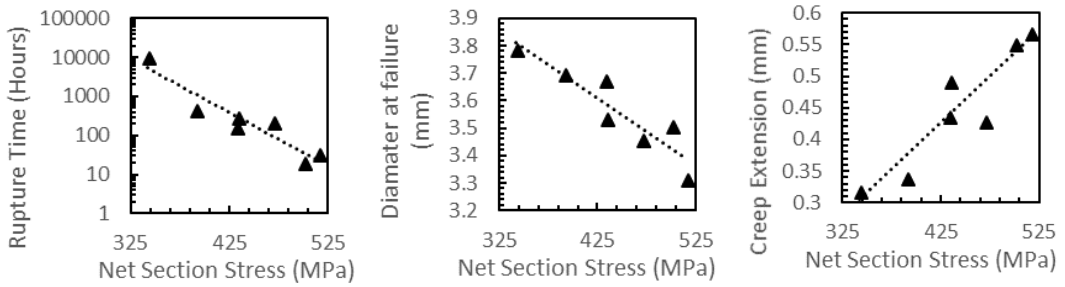

Figure 3(a,b,c) Rupture time, diameter on failure and extension during creep for various net section stresses (initial diameter 4mm for all specimens)

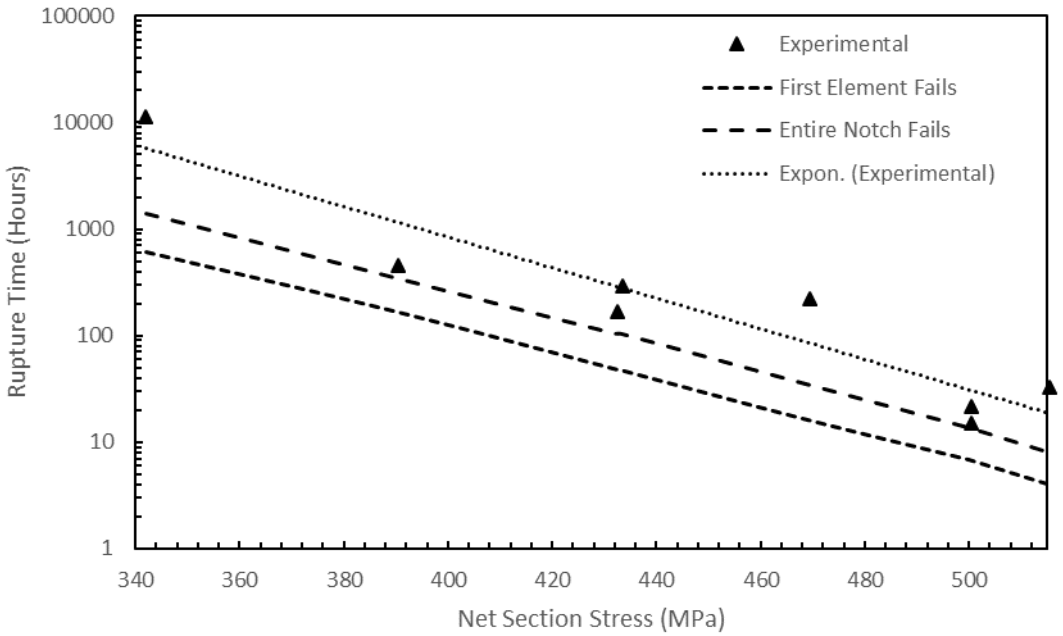

Figure 4- Rupture time vs net section stress (including FEA)

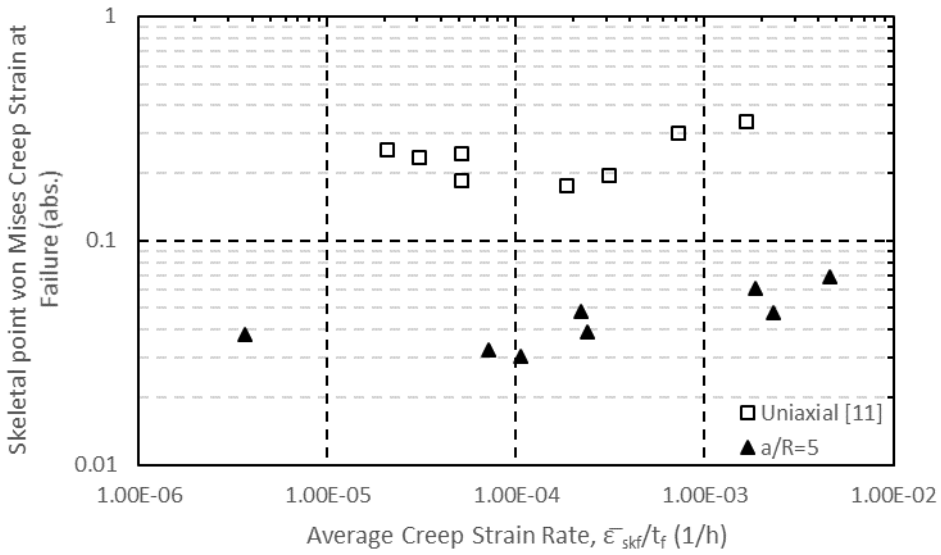

Figure 5 - Ductility of uniaxial and multiaxial specimens

The lower creep ductility and reduced plastic strain during the lower net section stress experiments is the reason for the reduced extension on failure and less of a reduction in diameter.

3.2 Numerical analysis

The results from the finite element model were compared with uniaxial creep data [24]. The model accurately predicted Elastic-Plastic Primary-Secondary (EP-PS) creep. The model accurately captured the creep behaviour of round bar specimens subject to constant load creep.

An elastic plastic simulation was conducted with the notched specimen, the hydrostatic, von Mises equivalent, maximum principal and net section stresses can be seen along the notched diameter in Figure 6. The stress triaxiality (Hydrostatic stress/Mises stress) and Spindler Fraction along the notched diameter can be seen in Figure 7.

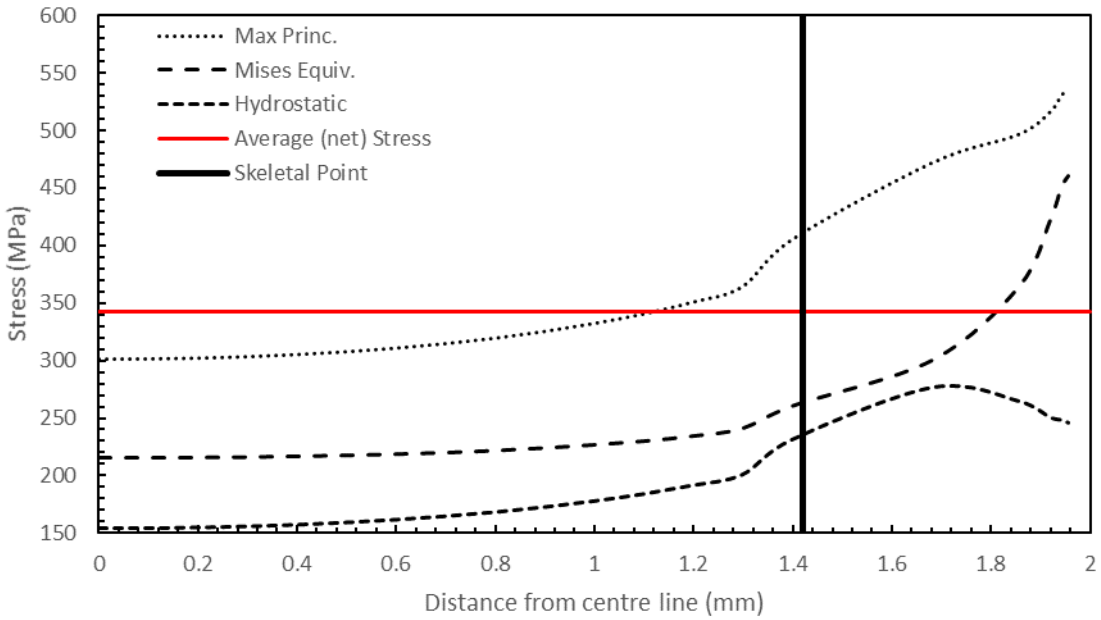

Figure 6 – Maximum principal, von Mises equivalent, hydrostatic and net section stresses along the centre line after loading up to 342MPa (no creep)

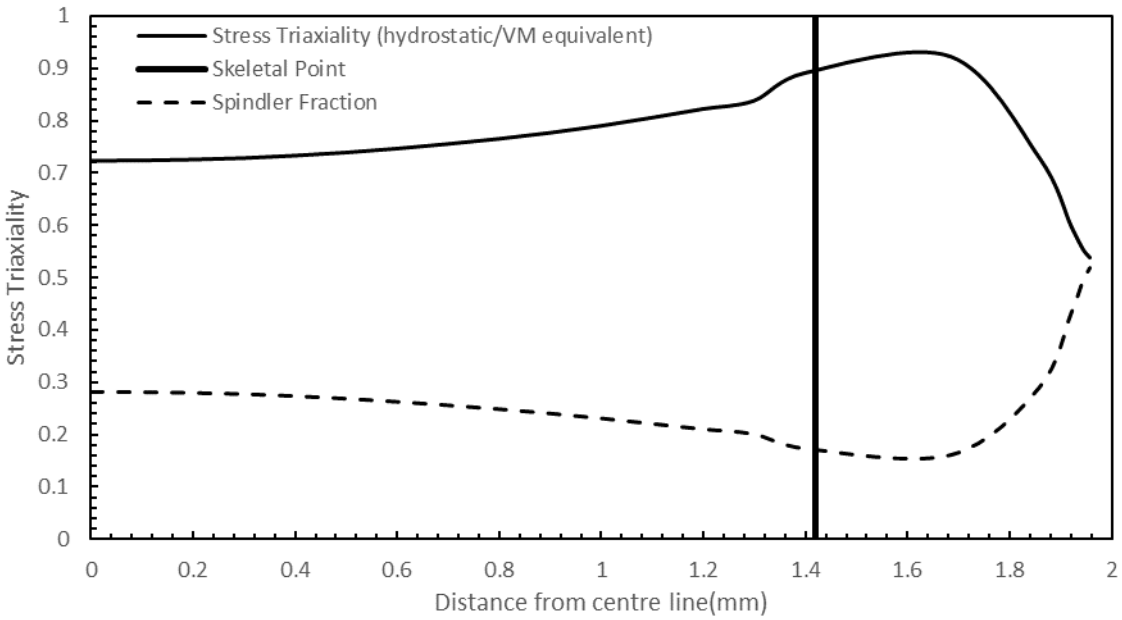

Figure 7 – Stress triaxiality and Spindler Fraction along the centre line after loading up to 342MPa (no creep)

Figure 8 shows extension against time for the test at 390MPa. Figure 8 shows that the experimental and FEA results were in good agreement regarding to extension at failure. The extension on failure was 2% higher in the experiment than the FEA, but the time to rupture was 28% longer in the experiment than the FEA. This showed the model was within the margin of error

expected within creep tests and on the conservative side (the two experiments conducted at 500MPa were 43% different in time to rupture).

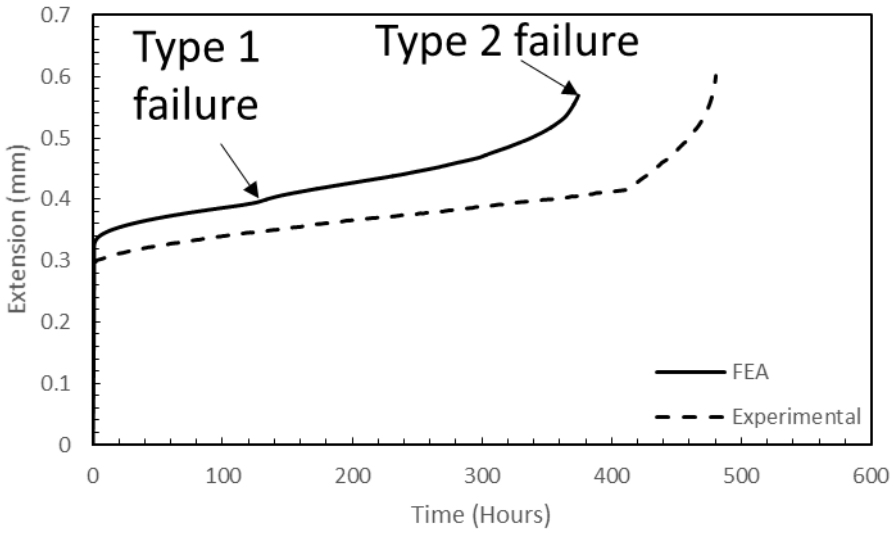

Figure 8 - Notched bar with applied net section stress 390MPa

Creep Damage

Figure 9 shows that in the finite element model the Mises creep strain on failure at the point of maximum damage increases with the average experimental Mises creep strain rate (defined here as failure strain/time to rupture).

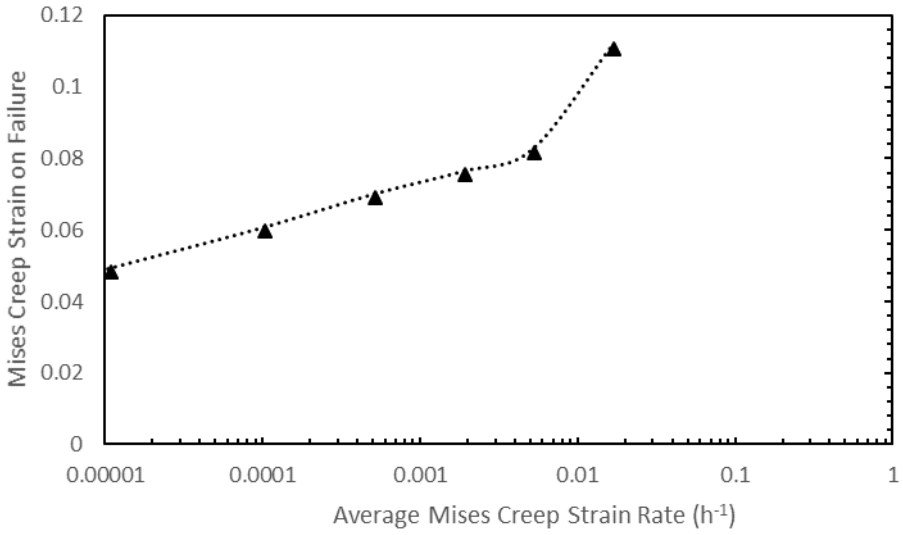

Figure 9- Mises creep strain on failure against average Mises creep strain rate (FEA) at the point of maximum damage

Figure 10 shows how damage is accumulated over time at the elements of maximum and minimum damage across the notch ligament. Type 1 failure is defined as when the element of

maximum damage reaches a damage value of 1. Type 2 failure is defined as when all elements along the notched diameter reach a damage value of 1.

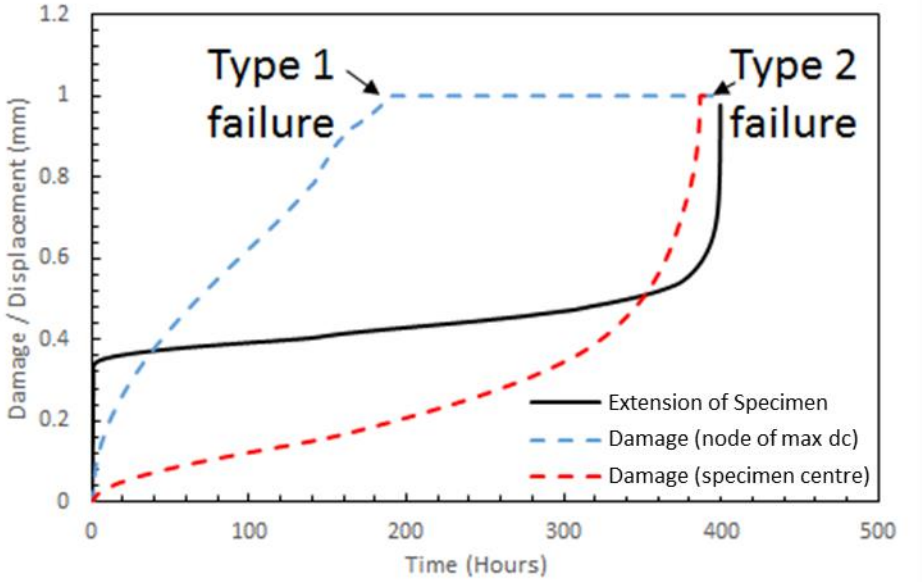

Figure 10 - Creep damage accumulation over time leading to failures (Net section stress 390MPa (FEA extension shown))

Figure 11 shows the distribution of creep damage across the notch ligament. Figure 11 predicts failure will have occurred at the surface earlier than it did at the Skeletal point. This agrees with previous notched bar FEA conducted by Spindler [24]. Other research on notched bars has used the Skeletal point as a focal point for analysis [30]. This shows that using the Skeletal point may give us an underestimate of creep damage at failure (assuming the damage model of equations 2 and 5).

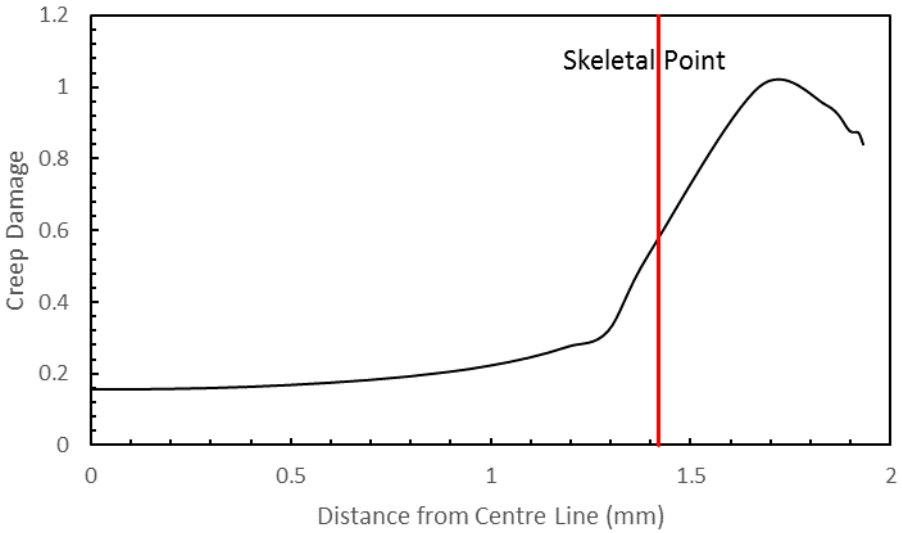

Figure 11 - Creep damage predicted across ligament as first element fails (Type 1 failure distribution)

Figure 12 shows the experimental reduction in diameter of this specimen compared with the reduction in diameter obtained from the finite element model, both plotted against time. From

this comparison, it can be seen that the reduction in diameter after loading up is captured very well by the finite element model as is the reduction in diameter during subsequent creep.

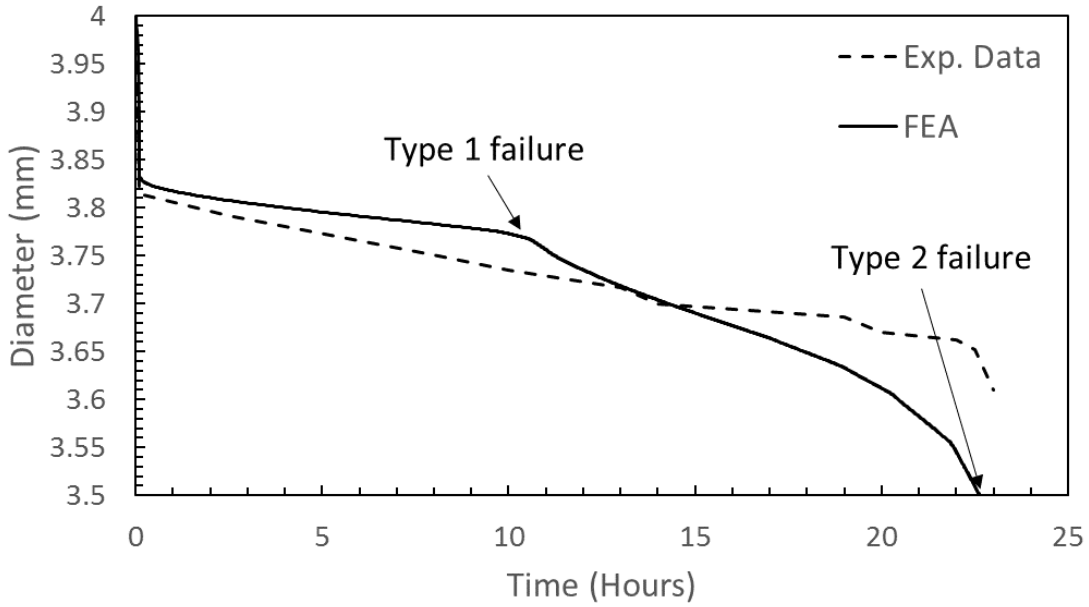

Figure 12 - Reduction in diameter, 500MPa net section stress (data from camera)

Figure 13 shows the notch opening of the same specimen from the same creep test (net section stress 500MPa, 550˚C) again plotted alongside the finite element simulation. Again, it can be seen that the finite element model accurately captures the behaviour of the specimen. Figure 13 shows how the overall extension of the specimen is predominantly coming from the notch. For the test with a 500MPa net section stress the overall extension on failure was 1.73mm of which 1.48mm was notch opening. 85% of the specimen's extension is from the notch, given that the notch only accounts for 3% of the overall length of the specimen it is clear that the notch is the area of greatest interest where the highest stresses and strains are apparent. This was confirmed by the experimental and finite element work.

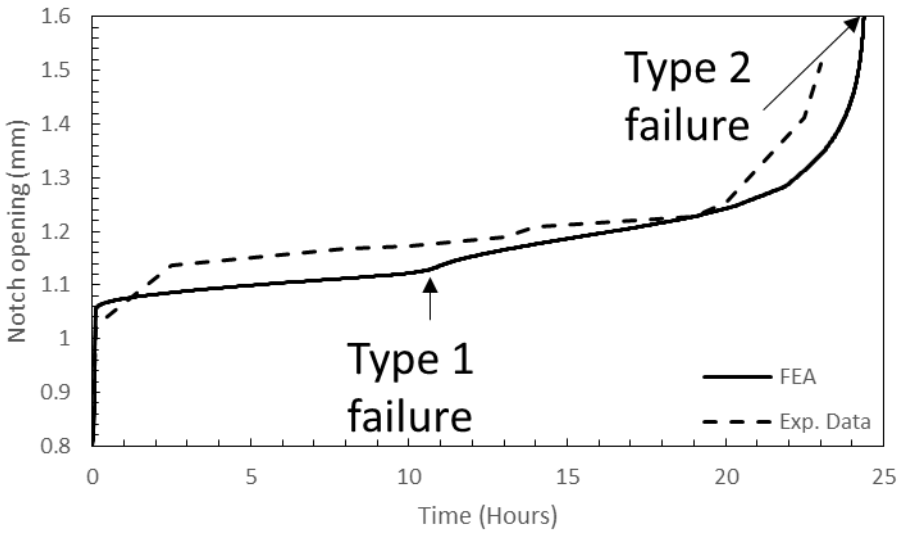

Figure 13- Notch opening, 500MPa net section stress

Figure 14 shows the final image captured before failure of the specimen from the experiment overlayed with the corresponding FEA simulation (500MPa net section stress). This Figure shows the deformation of the specimen was captured by the model and the damage throughout the specimen can be seen.

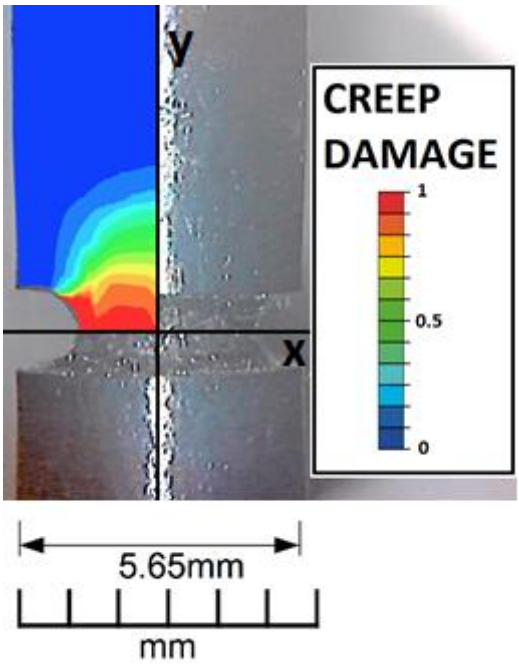

Figure 14- 500MPa net section stress test, FEA (Type 2 failure) and experimental (last image taken before failure of the specimen)

4. Discussion

Unsurprisingly, all the specimens failed at the notch. This was because the cross-sectional area was lowest at the notched section, so the net section stress was the highest at this area. Furthermore a small radius notch was used which generated a high stress concentration factor (approximately 3) and induced triaxiality, which together reduce the time to rupture in a specimen [31]. The triaxiality at the notch peaked after initial load, the ratio of hydrostatic to Mises stress being almost 3 times the value experienced in cylindrical specimens [5].

As the net section stress applied to the specimens was increased the time to rupture was decreased, the extension on load up was increased and the creep extension on failure was increased. This agrees with research conducted on similar materials that found that creep ductility is a function of stress, temperature and loading rates [12].

The finite element model used showed very good agreement with the experimental data in the case of uniaxial specimens. This was expected as the constants used in the FEA had been derived from the uniaxial test data. When the FEA was compared to the experimental results of the notched bar rupture tests it was found to be within the range of the experimental data but towards the conservative side rather than being the average as with the uniaxial data. Agree-

ment between the data and the model was strong with the model able to predict the notch opening and reduction in area of the notched specimen accurately when compared to the data obtained experimentally (with the camera set-up). The model found that damage reaches 1 (first element fails (Type 1 failure) approximately 40% of the way into the creep life of the specimen then propagates progressively faster through the specimen as creep continues until rupture of the specimen when all elements along the root of the notch fail (Type 2 failure).

The test results and the FEA are consistent with an approximately exponential relationship between stress and rupture time (Fig.4). A test was started with a net section stress of 260MPa on the same specimen geometry and was run for over 4,000 hours and was predicted to be approximately one tenth of the way through its creep life from the data till that point but a power shutdown in the lab interrupting the furnace and integrity of the specimen led to termination of the test before rupture of the specimen.

The creep strain at failure was almost twice as large for the higher stress tests than for the lower stress tests. This suggests that creep strain is not always equally damaging, the results suggest that for a fixed amount of creep strain, the slower it is accumulated the more damaging it is to the specimen. Previous work on this material has shown that prior plastic loading will lower the creep ductility of a specimen [32], suggesting that the tests conducted at a high load would have failed at a greater creep strain had there not been significant plastic strain at the notch during load up. This further confirms the view that creep strain is less damaging the faster it is accumulated in this material. This implies where damage is predicted from creep-fatigue cycles, and hence repeat relaxations, the initial, faster, phase of relaxation may be less damaging than the same strain accumulated slowly. Direct demonstration of this effect is the subject of ongoing work by the authors.

It has been postulated that the formation of creep voids/cavities are both stress and time dependent [9]. Using the Monkman-Grant relationship for predicting creep cavitation suggests that in the longer term lower stress creep tests, more cavities will form than in the short term higher stress tests. The resulting lower cavity spacing could explain the failures occurring at a lower creep ductility/extension in the lower stress tests. However, the experimental findings stand alone, independent of this proffered mechanistic explanation.

5. Conclusions

Nine experiments with varying net section stresses were conducted on notched bar specimens (All specimens had a notch acuity of 5). Notched bar specimens were used to introduce a stress triaxiality and reduce failure times. Finite element simulations were conducted using Abaqus to determine the behaviour at the notch of the specimens. The conclusions drawn from this work were that in creep rupture as the net section stress increases the time to failure reduces but the creep ductility on failure increases implying the material has a time or strain rate dependent creep ductility. As net section stress is increased the overall extension of the specimen on failure is increased and specimen diameter on failure is reduced. Moreover, the extension and diameter change attributable to creep also increase as the net section stress is increased, further confirming this material has an increased creep ductility at higher strain rates/stresses. As net section stress is increased, hoop and skeletal creep strains on failure are also increased. It has been shown that using creep constants derived from uniaxial creep data it is possible to accurately capture creep behaviour of notched bar specimens with a notch acuity of 5. The highest stress triaxiality factor (hydrostatic stress/Mises stress) occurs just away from the notch tip, 1.65mm from the centre line (15% of the distance from the edge of the notch to the centre line), the same point on the specimen where damage reaches 1 (unity) first. The higher the net section stress and therefore the higher the average creep strain rate in creep rupture tests, the

higher the extension and creep ductility of the specimens on failure. This leads to the key conclusion drawn from this work which is that a given creep strain is more damaging the slower it is accumulated in creep rupture of Type 316H stainless steel (i.e., components subject to lower strain rates will fail at reduced ductilities). Smaller effective creep ductilities may therefore apply at the very slow strain rates relevant to plant operating for several decades.

6. Acknowledgement
The authors would like to thank M. Spindler for his valuable advice regarding conducting the experimental work and for offering his wealth of knowledge on the subject and EDF Energy for use of their creep lab for two of the experiments conducted in this study.

7. References

1. Cocks ACF, Ashby MF. Intergranular Fracture during Power-Law Creep under Multiaxial Stresses. Met Sci. 1980;14(8-9):395-402.
2. Yatomi M, Bettinson AD, O'Dowd NP, Nikbin KM. Modelling of damage development and failure in notched-bar multiaxial creep tests. Fatigue Fract Eng M. 2004;27(4):283-95.
3. Hyde TH, Xia L, Becker AA. Prediction of creep failure in aeroengine materials under multi-axial stress states. Int J Mech Sci. 1996;38(4):385-+.
4. Hayhurst DR, Dimmer PR, Morrison CJ. Development of Continuum Damage in the Creep-Rupture of Notched Bars. Philos T R Soc A. 1984;311(1516):103-+.
5. Spindler MW. Creep behavior of ex-service Type 316H. Unpublished work.
6. Rice JR, Tracey DM. On Ductile Enlargement of Voids in Triaxial Stress Fields. J Mech Phys Solids. 1969;17(3):201-+.
7. Hales R. The Role of Cavity Growth Mechanisms in Determining Creep-Rupture under Multiaxial Stresses. Fatigue & Fracture of Engineering Materials & Structures. 1994;17(5):579-91.
8. Alfaddagh KD, Fenner RT, Webster GA. Steady-State Stress Distributions in Circumferentially Notched Bars Subjected to Creep. J Strain Anal Eng. 1982;17(3):123-32.
9. Hayhurst DR, Leckie FA, Henderson JT. Design of Notched Bars for Creep-Rupture Testing under Triaxial Stresses. Int J Mech Sci. 1977;19(3):147-59.
10. Hayhurst, Webster. An overview on studies of stress state effects during creep of circumferentially notched bars. , in: Gooch, DJ, How, IM, editors Techniques for multiaxial creep testing, Amsterdam: Elsevier, 137-143. 1986.
11. Spindler MW. The Multiaxial Creep of Austenitic Stainless Steels. Nuclear Electric Report TIGM/REP/0014/94. 1994.
12. Yatomi M. Modelling of damage development and failure in notched-bar multiaxial creep tests. Fatigue & Fracture of Engineering Materials & Structures 2004;27.4:283-95.
13. Takahashi Y, Shibamoto H, Inoue K. Long-term creep rupture behavior of smoothed and notched bar specimens of low-carbon nitrogen-controlled 316 stainless steel (316FR) and their evaluation. Nucl Eng Des. 2008;238(2):310-21.
14. Spindler MW. The multiaxial and uniaxial creep ductility of Type 304 steel as a function of stress and strain rate. Mater High Temp. 2004;21(1):47-54.
15. Spindler MW, Hales R, Skelton RP. The Multiaxial Creep Ductility of an Ex-Service Type 316H Stainless Steel. 9th International Conference on Creep and Fracture of Engineering Materials and Structures. 2001:679-88.
16. Oh CS, Kim NH, Kim YJ, Davies C, Nikbin K, Dean D. Creep failure simulations of 316H at 550 degrees C: Part I - A method and validation. Engineering Fracture Mechanics. 2011;78(17):2966-77.

17. Oh CS, Nah-Hyun Kim, Sung-Hwan Min, Kim Y-J. Finite Element Damage Analysis for Predictions of Creep Crack Growth. Proceedings of the ASME 2010 Pressure Vessels and Piping Division. 2010:1-5.
18. Spindler MW. The multiaxial creep ductility of austenitic stainless steels. Fatigue & Fracture of Engineering Materials & Structures. 2004;27(4):273-81.
19. Kachanov LM. Rupture time under creep conditions. Int J Fracture. 1999;97(1-4):Xi-Xviii.
20. Cane B. Creep Cavitation and Rupture in 2¼Cr1Mo Steel Under Uniaxial and Multiaxial Stresses. 3rd Int Conf on Mechanical Behaviour of Materials, Aug 1979, Cambridge; Proceedings Vol 2, pp 173-182, eds K J Miller & R F Smith, Pergamon Press, Oxford 1980.
21. RCC-MR. Section 1, Sub-section Z, Technical Appendix A3, AFCEN, Paris. 1985.
22. Stoter LP. Thermal Aging Effects in Aisi Type 316 Stainless-Steel. J Mater Sci. 1981;16(4):1039-51.
23. Norton F. The Creep of Steel at High Temperatures. McGraw-Hill, London 1929.
24. Spindler MW, Hales, R. and Skelton, R. P. The Multiaxial Creep Ductility of an Ex-Service Type 316H Stainless Steel. 9th International Conference on Creep and Fracture of Engineering Materials and Structures. 2001:679-88.
25. Webster GA, Holdsworth SR, Loveday MS, Nikbin K, Perrin IJ, Purper H, et al. A Code of Practice for conducting notched bar creep tests and for interpreting the data. Fatigue Fract Eng M. 2004;27(4):319-42.
26. Kassner ME, Hayes TA. Creep cavitation in metals. Int J Plasticity. 2003;19(10):1715-48.
27. Abaqus. Abaqus 6.14. [ONLINE] Available at: http://abaqus.software.polimi.it/v6.14/index.html. [Accessed 9 October 2017]. 2017.
28. Spindler MW, Smith MC. The effect of multiaxial states of stress on creep failure of Type 316h under displacement control. Proc PVP2009. 2009.
29. ASTM. Standard Methods for Tension Testing of Metallic Materials, ASTM E8 00b, Annual Book of ASTM Standards, Vol 03.01, West Conshohocken, PA, p56. 2001.
30. Webster GA, Nikbin KM, Biglari F. Finite element analysis of notched bar skeletal point stresses and dimension changes due to creep. Fatigue & Fracture of Engineering Materials & Structures. 2004;27(4):297-303.
31. Kang GZ, Kan QH, Zhang J, Sun YF. Time-dependent ratchetting experiments of SS304 stainless steel. Int J Plasticity. 2006;22(5):858-94.
32. Mehmanparast, Davies, Dean, Nikbin. Effects of plastic pre-straining level on the creep deformation, crack initiation and growth behaviour of 316H stainless steel. . Int J Pres Ves Pip. 2016;141:1-10.